

Laboratory Investigation of Vapor Shielding for Lithium-Coated Molybdenum in Devex

Soonwook Jung, Daniel Andruczyk, and David N. Ruzic

Abstract—To investigate the effect of lithium on a molybdenum target, a triple Langmuir probe diagnostics and target temperature measurements are carried out. Several experimental scenarios are tested to optimize the device for the vapor shielding experiment. A lithium sputtering system is used to deposit lithium on a molybdenum target. A triple Langmuir probe is placed near the target at various pressures to estimate change of plasma density and electron temperature and their effects on vapor shielding. Temperature increase at the target is measured by a thermocouple and its relationship with plasma parameters and lithium is discussed in detail.

Index Terms—Lithium, molybdenum, triple langmuir probe, vapor shielding.

I. INTRODUCTION

PLASMA-WALL interactions in fusion plasma reactors are becoming increasingly important because contact of hot plasma with the wall results in impairment to the wall and reduction of its lifetime. Some extreme events, such as edge localized mode and hard disruptions, caused high heat flux of plasma to be ejected to the chamber's wall and can severely damage the wall and plasma energy confinement. Such events are considered major obstacles to a successful fusion device.

Among possible candidates for the wall material, lithium has drawn scientific interest for its high chemical affinity and low recycling of hydrogen [5]. Computational and experimental studies of intense, pulsed plasma interactions with materials such as beryllium, lithium, carbon, and tungsten are being carried out. The results predicted that during the early stage of an intensive power deposition on a target material, a vapor cloud from the target debris will form above the bombarded surface [6]–[12]. Since lithium has more vaporization effect than other materials because of its high vapor pressure and low melting point, the vapor cloud from the lithium may further reduce the net energy flux to the originally exposed target surface and diminish the effect of plasma-wall interaction. While there is a concern that evaporation of lithium on molybdenum at a high evaporation rate may expose molybdenum to high heat flux and introduce high-*z* impurity into plasma, molybdenum has a good chemical compatibility with lithium.

The vapor shielding study of lithium-coated molybdenum will provide a better understanding of its applicability to the fusion reactor wall.

Because studying plasma-wall interactions in tokamaks is cost ineffective and time consuming, a number of test devices have been developed [9]–[18]. The necessity has also motivated at University of Illinois at Urbana-Champaign the development of a laboratory-scale experimental device to explore such potentially critical design problems that have arisen in the tokomaks. A facility called Divertor Erosion and Vapor Shielding eXperiment (DEVeX) facility was built to produce energetic plasma and to study plasma-material interactions in detail [19], [20] The DEVeX device is a laboratory-scale theta pinch which creates and compresses the plasma to reach conditions similar to fusion plasma conditions suitable for studying the impact of edge plasma on the first wall and diverter. In this device, the end-loss plasma from the theta pinch simulates energetic plasma exposure to a target.

Previous experiments in DEVeX have shown that plasma density and electron temperature reach 10^{21} m^{-3} and 10–100 eV, respectively, near the end of theta coil [2], [19]. However, the target chamber is approximately 65 cm away from the close end of the theta coil, which allows the plasma to expand as the energetic plasma is transported to the target. Moreover, this device requires installing a reliable preionization source at low pressure. Therefore, in this study, various operating scenarios resulting from system upgrades are tested to optimize the device for vapor shielding experiment. To observe the effect of addition of lithium and to understand its phenomenon, a molybdenum target will be exposed to heat flux of the plasma, and its temperature changes for different plasma conditions are compared. To physically understand the change of temperature, triple Langmuir probe diagnostics are carried out, and relation of the data to the lithium coating on the target is discussed.

II. EXPERIMENTAL SETUP

The main component of the experimental setup is the theta pinch device which generates hot and dense plasma. Fig. 1 shows the schematic of the experimental setup. A single-turn, four-segmented theta coil has a conically tapered angle of 1° to preferentially drive the plasma into a target region where a sample is located. In order to have high current flow through the theta coil, the coil is connected through 15 RG-19 coaxial cables to 18 parallel-connected capacitors. The main capacitors have total capacitance of 36 μF and can be charged up to 30 kV. In this paper, the charging voltage is fixed at 20 kV, yielding 7.2-kJ energy in the capacitors. When the bank is charged to

Manuscript received August 13, 2011; revised December 14, 2011; accepted December 20, 2011. Date of publication February 3, 2012; date of current version March 9, 2012.

The authors are with Nuclear, Plasma, and Radiological Engineering, University of Illinois at Urbana-Champaign, Urbana, IL 61801 USA (e-mail: druzic@illinois.edu).

Color versions of one or more of the figures in this paper are available online at <http://ieeexplore.ieee.org>.

Digital Object Identifier 10.1109/TPS.2011.2181980

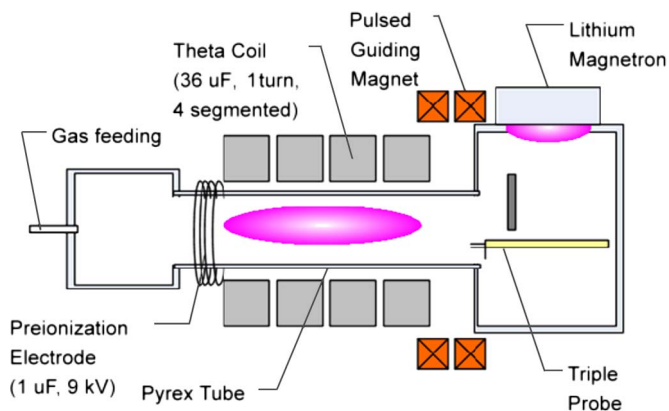


Fig. 1. Schematic of the DEVeX experimental setup.

20 kV, a pulse lasts for 80 μs and produces a magnetic field up to 0.7 T at the center of the coil.

A triple Langmuir probe [1]–[4] is located in the target chamber to measure electron temperature and plasma density at the position where the molybdenum target is located. The size of each tip is 0.25 mm in diameter and 2.5 mm in length. With 10 mTorr, 10^{19} m^{-3} and 10 eV, the probe size corresponds to collisionless thin sheath regime, according to [21]. A 100-Ohm current limiting resistor is connected with the triple Langmuir probe to measure the current flowing through the probe. The P2220 Tektronix 10:1 probes and the P5200 Tektronix 50:1 high voltage differential probes measure at the triple Langmuir probe circuit voltages of the probe. These are converted to plasma density and electron temperature. An external voltage source of approximately 65 V composed of 9-V batteries provides the bias voltage to the triple Langmuir probe.

The time of flight technique using a visible-wavelength-detectable photodiode is used to measure average plasma flow velocity toward the target chamber. The photodiodes are located at two different positions to measure average velocity between the two points. This technique is chosen as it is much simpler than using Mach or quadruple probes and yields accurate measurement of the average flow velocity.

The 55 mm wide, 52 mm long, and 0.076 mm thick molybdenum target has a K-type thermocouple bead spot welded on its back surface to measure temperature increase. A commercially available magnetron is used to deposit lithium onto the molybdenum sheet. A lithium target for the magnetron is fabricated in an argon-filled box to reduce its reaction with air and is discharge cleaned for 30 min to sputter off the remaining lithium compounds on the target. The deposition process is carried out at 300-V, 250-mA discharge voltage and current for an hour. The distance between the magnetron and the molybdenum target is less than 1 cm so that most of the sputtered lithium from the magnetron is deposited on the molybdenum. Assuming 100% deposition to the target, the thickness of the lithium coating is approximately 1–2 μm .

In order to increase incident heat flux to the target, several upgrades have been applied to the device. A four-turn copper electrode is connected to 1 μF capacitor through a spark gap switch to generate background plasma via inductively coupled

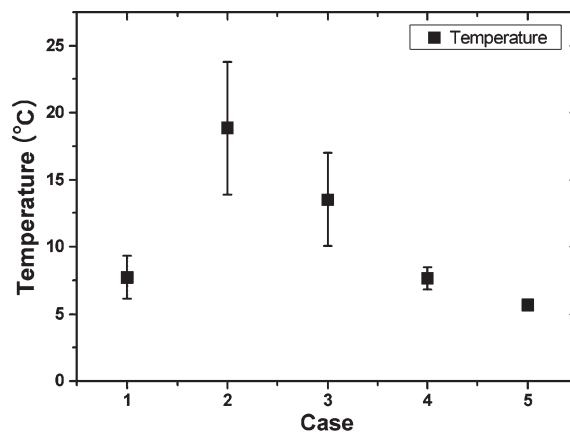


Fig. 2. Temperature increase at the target with various operating scenarios shows that the second case gives highest temperature increase. (case 1: only theta coil, case 2: preionization and theta coil, case 3: preionization, theta coil and magnet, case 4: preionization, theta coil, and crowbar, case 5: preionization, theta coil, magnet and crowbar).

plasma generation. This preionization electrode is fired 30 μs before the main capacitors to the theta coil is triggered.

Second, six stacks of 175-turn magnets are added between the theta coil and the target chamber to sustain magnetic field and keep the plasma compressed. A 4-mF capacitor is connected through a 50RIA60 SCR switch and produces 140-A peak current 12 ms after it was triggered. This current, measured by a calibrated Rogowski coil, corresponds to a magnetic field of approximately 0.2 T.

The last upgrade is the addition of a crowbar switch to manipulate the current waveform so that the theta coil current reaches its peak when the crowbar is closed. Without the crowbar, current at the theta coil is oscillating with time, resulting in continuous compression and decompression of the plasma. The gap of a railgap-type crowbar switch is finely adjusted to reproducibly operate when the main capacitor bank is charged to 20 kV and to prevent an inadvertent trigger because of a high electric field across the gap. Independent control and synchronization of the theta coil discharge, preionization discharge, magnet, and the crowbar triggering is achieved by Maxwell 40150 trigger generator. A hydrogen gas is used for this experiment, and pressure is varied from 1 to 10 mTorr.

III. RESULTS

A. Operation Scenario Test

Fig. 2 shows temperature increases at the molybdenum target with various operating scenarios. Unlike the initial expectation, the second case shows the maximum energy increase. It is attributed to the fact that the crowbar switch still has finite inductance and resistance which results in faster oscillations of the current instead of the current ceasing at the moment when the crowbar is triggered. Because of the oscillation, the directions of magnetic field at the theta coil and the magnet oppose to each other at the second $\lambda/2$, preventing plasma transport to the target region. However, the preionization source definitely increases the energy flux to the target, implying that the preionization source enhances power transfer efficiency.

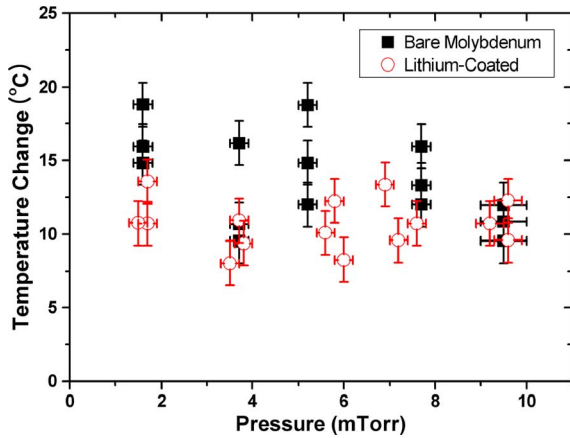


Fig. 3. Incident energy measurement for bare molybdenum (solid square dot) and lithium-coated molybdenum (empty circle dot) indicates reduction in the energy at low pressure.

Therefore, for the remaining work, only the preionization source and the capacitors to the theta coils are used.

B. Observation of Vapor Shielding at the Target

Fig. 3 shows temperature increases of the target with and without a lithium coating at various pressures. Although the energy stays around 10 J, very short pulse duration gives very high heat flux to the target, reaching up to 45 MW/m^2 . The pressure dependency is hard to see at high pressure around 10 mTorr, while at around $1.7 \pm 0.2 \text{ mTorr}$, lithium coating gives rise to energy difference of $2.7 \pm 1.7 \text{ J}$.

Vapor shielding is caused by formation of a vapor cloud from lithium either by sputtering or by evaporation. Evaporation is highly dependent on the surface temperature of the target, and its effects are negligible below the melting temperature of lithium. While it is extremely difficult to experimentally measure surface temperature of a target without dual-band infrared thermography [22] and thermocouples have very slow response time, an approximation of calibration factor for measured temperature of a target and the surface temperature using a thermal response model [19] gives a rough estimation of the surface temperature of the molybdenum target.

The analysis in Fig. 4 shows that the surface temperature for the molybdenum is approximately 1.3 times higher than the peak temperature measured by the thermocouple, while the calibration factor for stainless steel has a value of 9.5 [19]. This result is in agreement with thermal diffusion time which is approximately $100 \mu\text{s}$ for molybdenum and $1400 \mu\text{s}$ for stainless steel. This difference is attributed to the fact that molybdenum has much higher thermal conductivity and less heat capacity than stainless steel. Taking into consideration the calibration factor, the maximum temperature increase is less than $30 \text{ }^\circ\text{C}$, showing that evaporation is negligible in this case.

C. Validation of Triple Langmuir Probe Diagnostics

Before physically analyzing the possible cause of the vapor shielding with triple Langmuir probe, a simple verification of the reasonability of triple Langmuir probe data is necessary.

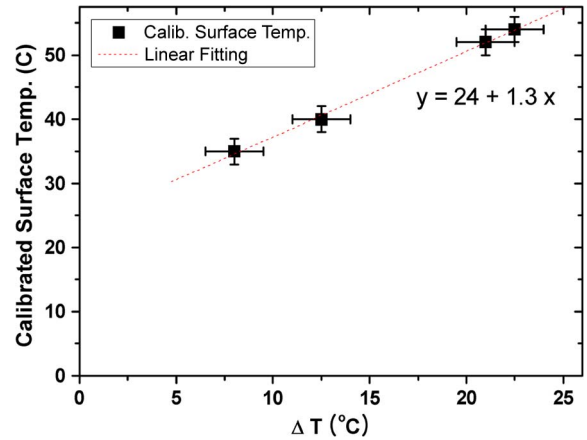


Fig. 4. Surface temperature estimation by a thermal response model [19] implies that the temperature increase is lower than evaporation temperature of lithium and contribution of lithium evaporation on vapor shielding for this experiment is negligible.

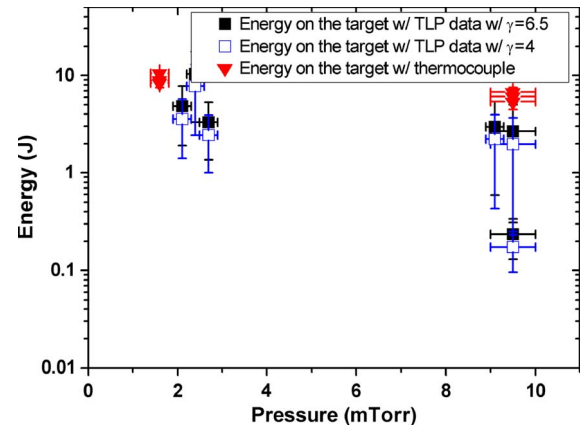


Fig. 5. Incident energy on the target estimated by triple Langmuir probe data with $\gamma = 6.5$ (solid square) and $\gamma = 4.8$ (empty square) show the similar behavior as the actual temperature increase measured by thermocouple (triangle).

While triple Langmuir probe allows the plasma parameters to be obtained as a function of time, the fluctuation of the electron temperature during the pulse duration due to periodic compression and decompression of the plasma creates problems for obtaining results. A requirement for an asymptotic solution is that the applied voltage at triple Langmuir probe be at least five times greater than the electron temperature for a solution. This is hard to guarantee with an oscillating electron temperature. Therefore, in the case of nonsaturation [23], the nonlinear equations in [1] should be solved in a nonalgebraic way. Moreover, measuring data that yields a high electron temperature is subject to a low signal-to-noise ratio, so that even small error in voltage signal ends up with very large error in density and temperature calculation. Therefore, a series of equations for error propagation are included in data analysis, and $\pm 0.5 \text{ V}$ error is considered in triple Langmuir probe measurement.

In order to verify the reasonability of triple Langmuir probe data, a comparison between transferred energy to the target measured by thermocouple and by the triple Langmuir probe

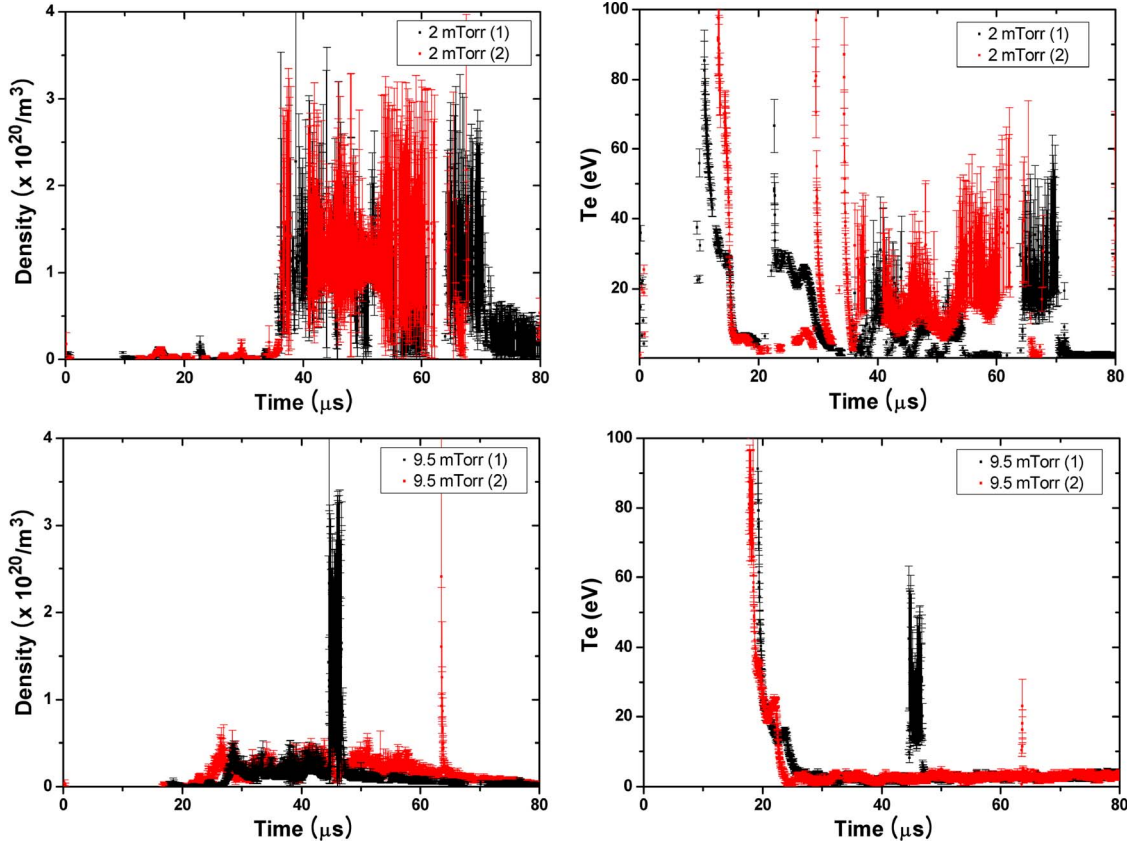


Fig. 6. Temporal behavior of (left) plasma density and (right) electron temperature (top) at 2 mTorr and (bottom) at 10 mTorr with two shots at each pressure. Black and red dots indicates two independent experiments at the same condition.

is carried out. The incident energy to the target is calculated with parameters from triple Langmuir probe using

$$E = \int_0^{t_0} \gamma n_e v A T_e dt \quad (1)$$

where γ is the heat transfer coefficient defined in [24] assuming that secondary electron emission is negligible, n_e plasma density, v plasma flow velocity measured by the time of flight technique, A the area of the target, T_e electron temperature, and t_0 the pulse duration. When ion and electron temperatures are equal, γ is 6.5, while when $T_i \ll T_e$, γ drops to 4.8. Therefore, two different values of γ have been plotted in Fig. 5. While the approach has many assumptions and the triple Langmuir probe analysis contains a large degree of error, Fig. 5 shows that energy calculated using (1) and thermocouple data are on the same order.

D. Triple Langmuir Probe Parameter Analysis

Fig. 6 shows temporal behaviors of plasma density and electron temperature measured by triple Langmuir probe at 2-mTorr and 10-mTorr pressure. At 10 mTorr, electron temperature stays almost constant with one peak. The 2-mTorr case shows more fluctuations in the density and temperature. This difference results from the fact that plasma suffers more collision at higher pressure as they are transported to the target and lose their energy to the nearby particles. Moreover, the larger population

of high energy particles implies that more sputtering takes place at the lithium surface, for sputtering yield of lithium [19], [25] by hydrogen ion bombardment increases rapidly between 10 eV and 100 eV.

Plasma flow velocity measured by time of flight technique is estimated $2.6 \pm 0.6(10)^4$ m/s at 2 mTorr and $1.3 \pm 0.1(10)^4$ m/s at 10 mTorr. The difference of the flow velocities is less than a few eV, which has very little effect on enhancement of lithium sputtering. Therefore, instant electron temperature and plasma density have significant larger effect on the vapor shielding observed in this experiment and the vapor shielding effect becomes more significant at the low pressure.

IV. CONCLUSION

In order to study vapor shielding effect in DEVeX, several device upgrades are carried out, and several operating scenarios are tested. It has been shown that the best achieved heat flux to the target is with the use of preionization. Temperature measurements at a molybdenum target by thermocouple indicate lithium deposition on the surface may reduce heat load from 9.7 ± 1.0 J to 7.0 ± 0.7 J at 2 mTorr, yielding energy difference of 2.7 ± 1.7 J, while difference at high pressure is undistinguished. Surface temperature analysis shows that vapor generation by the evaporation process is negligible, and triple Langmuir probe and time of flight diagnostics indicates that the difference dependent on pressure mainly results from higher instant plasma density and electron temperature of plasma to

the target, which gives rise to higher sputtering yield and formation of denser vapor cloud.

ACKNOWLEDGMENT

The research reported in this paper was performed in support of contract number DE-FG02-04ER54765 with the U.S. Department of Energy and Oak Ridge National Laboratory. The author would like to thank M. Williams for numerous technical discussions and undergraduate researchers L. A. Kesler, H. H. Yun, and B. Sherred for their time and commitment in the laboratory.

REFERENCES

- [1] S. Chen and T. Sekiguchi, "Instantaneous direct-display system of plasma parameters by means of triple probe," *J. Appl. Phys.*, vol. 36, no. 8, pp. 2363–2375, Aug. 1965.
- [2] S. Jung, V. Surla, T. K. Gray, D. Andruczyk, and D. N. Ruzic, "Characterization of a theta-pinch plasma using triple probe diagnostic," *J. Nucl. Mater.*, vol. 415, no. 1, pp. S993–S995, Aug. 2011.
- [3] T. K. Gray, M. A. Jaworski, and D. N. Ruzic, "Target heat loading due to fast, transient heat pulses produced from a conical θ -pinch as a prototype for benchmarking simulations of transient heat loads," *J. Nucl. Mater.*, vol. 363–365, pp. 1032–1036, Jun. 2007.
- [4] N. A. Gatsonis, L. T. Byrne, J. C. Zwahlen, E. J. Pencil, and H. Kamhawi, "Current-mode triple and quadruple Langmuir probe methods with applications to flowing pulsed plasmas," *IEEE Trans. Plasma Sci.*, vol. 32, no. 5, pp. 2118–2129, Oct. 2004.
- [5] R. Majeski, "Liquid metal walls, lithium, and low recycling boundary conditions in tokamaks," *AIP Conf. Proc.*, vol. 1237, no. 1, pp. 122–137, Jan. 2010.
- [6] A. Hassanein, "Prediction of material erosion and lifetime during major plasma instabilities in tokamak devices," *Fusion. Eng. Des.*, vol. 60, no. 4, pp. 527–546, Jul. 2002.
- [7] A. Hassanein and I. Konkashbaev, "An assessment of disruption erosion in the ITER environment," *Fusion. Eng. Des.*, vol. 28, pp. 27–33, Mar. 1995.
- [8] A. Hassanein and I. Konkashbaev, "Comprehensive modeling of ELMs and their effect on plasma-facing surfaces during normal tokamak operation," *J. Nucl. Mater.*, vol. 313–316, pp. 664–669, Mar. 2003.
- [9] H. Würz, N. I. Arkipov, V. P. Bakhtin, B. Goel, W. Höbel, I. Konkashbaev, I. Landman, G. Piazza, V. M. Safronov, A. R. Sherbakov, D. A. Toporkov, and A. M. Zhilukhin, "Numerical modeling and experimental simulation of vapor shield formation and divertor material erosion for ITER typical plasma disruptions," *J. Nucl. Mater.*, vol. 212–215, pp. 1349–1352, Sep. 1994.
- [10] M. A. Bourham, O. E. Hankins, O. Auciello, J. M. Stock, B. W. Wehring, R. B. Mohanti, and J. G. Gilligan, "Vapor shielding and erosion of surfaces exposed to a high heat load in an electrothermal accelerator," *IEEE Trans. Plasma Sci.*, vol. 17, no. 3, pp. 386–391, Jun. 1989.
- [11] J. T. Bradley, III, J. M. Gahl, and P. D. Rockett, "Diagnostics and analysis of incident and vapor shield plasmas in PLADIS I, A coaxial deflagration gun for Tokamak disruption simulation," *IEEE Trans. Plasma Sci.*, vol. 27, no. 4, pp. 1105–1114, Aug. 1999.
- [12] M. A. Bourham and J. G. Gilligan, "Erosion of plasma-facing components under simulated disruption-like conditions using an electrothermal plasma gun," *Nucl. Technol.*, vol. 26, no. 3, pp. 517–521, Nov. 1994.
- [13] V. R. Barabash, A. G. Baranov, J. Gahl, V. L. Litunovsky, J. McDonald, and I. B. Ovchinnikov, "Experimental study of pulse plasma-carbon materials interaction during the simulation of thermal quench phase of tokamak plasma disruption," *J. Nucl. Mater.*, vol. 187, no. 3, pp. 298–302, Mar. 1995.
- [14] P. D. Rockett, J. A. Hunter, J. M. Gahl, J. T. Bradley, III, and R. R. Peterson, "Plasma gun experiments and modeling of disruptions," *J. Nucl. Mater.*, vol. 212–215, pp. 1278–1282, Sep. 1994.
- [15] J. M. Gahl, J. M. McDonald, A. Zakharov, S. Tseremitinov, V. Barabash, and M. Guseva, "Heat load material studies: Simulated tokamak disruptions," *Fusion Eng. Des.*, vol. 191–194, pp. 454–459, Sep. 1992.
- [16] N. I. Arkipov, V. P. Bakhtin, S. M. Kurkin, V. M. Safronov, D. A. Toporkov, S. G. Vasenin, A. M. Zhilukhin, and H. Würz, "Material erosion and erosion products in disruption simulation experiments at the MK-200 UG facility," *Fusion Eng. Des.*, vol. 49–50, pp. 151–156, Nov. 2000.
- [17] H. Würz, S. Pestchanyi, I. Landman, B. Bazylev, V. Tolkach, and F. Kappler, "A 2-D numerical simulation of ITER-FEAT disruptive hot plasma-wall interaction and model validation against disruption simulation experiments," *Fusion Sci. Technol.*, vol. 40, pp. 191–246, Nov. 2001.
- [18] V. G. Belan, V. F. Levashov, V. S. Maynashev, A. D. Muzichenko, and V. L. Podkovirov, "Features of dynamics and structure of the shielding layer at the interaction of plasma flow with target," *J. Nucl. Mater.*, vol. 233–237, pp. 763–766, Oct. 1996.
- [19] T. Gray, "Bombardment of thin lithium films with energetic plasma flows," Ph.D. dissertation, Univ. Illinois, Urbana-Champaign, IL, 2009.
- [20] T. Gray, M. Williams, and D. N. Ruzic, "Overview and status of the divertor erosion and vapor shielding eXperiment (DEVeX)," in *Proc. IEEE 22nd Symp. Fusion Eng.*, Jun. 2007, pp. 1–4.
- [21] D. N. Ruzic, *Electric Probes for Low Temperature Plasmas*. New York: AVS Press, 1994, pp. 12–16.
- [22] J. Kallman, M. A. Jaworski, R. Kaita, H. Kugel, A. McLean, and V. Surla, "Determination of effective sheath heat transmission coefficient in NSTX discharges with applied lithium coating," presented at the 2nd Int. Symp. Lithium Applications Fusion Devices, Princeton, NJ, Apr., 2011.
- [23] M. Laux, "How to interpret triple probe measurements when non of the tips saturates?" *Contrib. Plasma Phys.*, vol. 44, no. 7/8, pp. 695–699, Nov. 2004.
- [24] J. Wesson, *Tokamaks*, 3rd ed. Oxford, U.K.: Clarendon, 2004, pp. 446–449.
- [25] J. P. Allain and D. N. Ruzic, "Measurements and modelling of solid phase lithium sputtering," *Nucl. Fusion*, vol. 42, no. 2, pp. 202–210, Feb. 2002.



Soonwook Jung received the B.S. and M.S. degrees in nuclear engineering from Seoul National University, Seoul, Korea in 2006 and 2008, respectively. He is currently working toward the Ph.D. degree at the Department of Nuclear, Plasma, Radiological Engineering, University of Illinois at Urbana Champaign, Urbana.

After M.S. degree, he worked as an Assistant Researcher in Center for Advance Research in Fusion Reactor Engineering. His research interests include plasma-surface interaction, pulse power system, pulse plasma diagnostic, and high voltage breakdown.



Daniel Andruczyk received the Ph.D. degree in physics from The University of Sydney, Sydney, NSW, Australia, in 2006.

He is a Postdoc in the Department of Nuclear, Plasma, and Radiological Engineering, University of Illinois, Urbana. He joined the staff, in 2010. After receiving his Ph.D. degree, he did one postdoctoral at the Max-Planck Institute for Plasma Physics, Greifswald on the WEGA Stellarator. His research centers on the interaction of plasmas with materials as well as plasma diagnostics applications include

magnetic fusion energy, as well as microelectronic and plasma processing.



David N. Ruzic received the Ph.D. degree in physics from Princeton University, Princeton, NJ, in 1984.

He is the Director of the Center for Plasma Material Interactions at the University of Illinois at Urbana-Champaign, Urbana. He is a professor in the Department of Nuclear, Plasma, and Radiological Engineering and affiliated with the Department of Electrical and Computer Engineering and the Department of Physics, having joined the faculty, in 1984. His current research interests center on plasma processing for the microelectronics industry (deposition, etching, EUV lithography, and particle removal), atmospheric-pressure plasmas for industrial applications, and on fusion energy research. He has a passion for teaching, particularly about energy sources, because he gets to blow something up in almost every class.

Dr. Ruzic is a Fellow of the American Nuclear Society and of the American Vacuum Society.